

Postprint of: Potęga A., Żelaszczyk D., Mazerska Z., Electrochemical simulation of metabolism for antitumor-active imidazoacridinone C-1311 and *in silico* prediction of drug metabolic reactions, Journal of Pharmaceutical and Biomedical Analysis, Vol. 169 (2019), pp. 269-278, DOI: [10.1016/j.jpba.2019.03.017](https://doi.org/10.1016/j.jpba.2019.03.017)

© 2019. This manuscript version is made available under the CC-BY-NC-ND 4.0 license  
<http://creativecommons.org/licenses/by-nc-nd/4.0/>

#### Research highlights

- Phase I metabolism of C-1311 was successfully simulated in an electrochemical cell.
- The products of *N*-dealkylation and aliphatic hydroxylation reactions were detected.
- *In silico* analysis was used for the prediction of P450-mediated metabolites.
- We observed a good accordance between electrochemical and *in silico* results.
- Electrochemical and *in silico* methods are fast alternatives for enzymatic assays.

1 **Title page**

2

3 **Title:**

4 Electrochemical simulation of metabolism for antitumor-active imidazoacridinone C-1311 and  
5 *in silico* prediction of drug metabolic reactions.

6

7 **Authors:**

8 Agnieszka Potęga <sup>a</sup>, Dorota Żelaszczyk <sup>b</sup>, Zofia Mazerska <sup>a</sup>

9

10 **Affiliations:**

11 <sup>a</sup> Department of Pharmaceutical Technology and Biochemistry, Faculty of Chemistry, Gdańsk  
12 University of Technology, Gabriela Narutowicza St. 11/12, Gdańsk 80-233, Poland.

13 agnieszka.potega@pg.edu.pl (A.P.), zofia.mazerska@pg.edu.pl (Z.M.)

14 <sup>b</sup> Department of Organic Chemistry, Faculty of Pharmacy, Jagiellonian University, Medyczna  
15 St. 9, Kraków 30-688, Poland.

16 dorota.zelaszczyk@uj.edu.pl (D.Ż.)

17

18 **Corresponding author:**

19 Agnieszka Potęga

20 Department of Pharmaceutical Technology and Biochemistry, Faculty of Chemistry, Gdańsk  
21 University of Technology, Gabriela Narutowicza St. 11/12, Gdańsk 80-233, Poland.

22 e-mail: agnieszka.potega@pg.edu.pl, telephone: +48 58 347 15 93, fax: +48 58 347 11 44

23 **Abstract**

24 The metabolism of antitumor-active 5-diethylaminoethylamino-8-hydroxyimidazoacridinone  
25 (C-1311) has been investigated widely over the last decade but some aspects of molecular  
26 mechanisms of its metabolic transformation are still not explained. In the current work, we have  
27 reported a direct and rapid analytical tool for better prediction of C-1311 metabolism which is  
28 based on electrochemistry (EC) coupled on-line with electrospray ionization mass  
29 spectrometry (ESI-MS). Simulation of the oxidative phase I metabolism of the compound was  
30 achieved in a simple electrochemical thin-layer cell consisting of three electrodes (ROXY™,  
31 Antec Leyden, the Netherlands). We demonstrated that the formation of the products of *N*-  
32 dealkylation reactions can be easily simulated using purely instrumental approach. Newly  
33 reported products of oxidative transformations like hydroxylated or oxygenated derivatives  
34 become accessible. Structures of the electrochemically generated metabolites were elucidated  
35 on the basis of accurate mass ion data and tandem mass spectrometry experiments. *In silico*  
36 prediction of main sites of C-1311 metabolism was performed using MetaSite software. The  
37 compound was evaluated for cytochrome P450 1A2-, 3A4-, and 2D6-mediated reactions. The  
38 results obtained by EC were also compared and correlated with those of reported earlier for  
39 conventional *in vitro* enzymatic studies in the presence of liver microsomes and in the model  
40 peroxidase system. The *in vitro* experimental approach and the *in silico* metabolism findings  
41 showed a quite good agreement with the data from EC/ESI-MS analysis. Thus, we conclude  
42 here that the electrochemical technique provides the promising platform for the simple  
43 evaluation of drug metabolism and the reaction mechanism studies, giving first clues to the  
44 metabolic transformation of pharmaceuticals in the human body.

45  
46 **Keywords:** Antitumor compound; On-line electrochemistry-mass spectrometry; Metabolite  
47 electrosynthesis; *In silico* site of metabolism prediction; Cytochrome P450; *In vitro* drug  
48 metabolism;



49 **Abbreviations**

50 C-1311, 5-diethylaminoethylamino-8-hydroxyimidazoacridinone; EC, electrochemistry,  
51 electrochemical; ESI, electrospray ionization; FA, formic acid; LC, liquid chromatography; *m/z*,  
52 mass-to-charge ratio; MS, mass spectrometry, mass spectrometer; MW, molecular weight;  
53 MS/MS, tandem mass spectrometry; P450, cytochrome P450; Q-TOF, quadrupole-time of  
54 flight

55

56 Parts of this work were presented at the 3<sup>rd</sup> International Summit on Toxicology & Applied  
57 Pharmacology (Chicago, IL, USA, 2014), at the 13<sup>th</sup> European ISSX Meeting (Glasgow,  
58 Scotland, 2015), and at the 20<sup>th</sup> North American ISSX Meeting (Orlando, FL, USA, 2015).

## 59 1. Introduction

60 Imidazoacridinones represent a group of the promising antitumor-active compounds  
61 developed in our laboratory [1]. 5-Diethylaminoethylamino-8-hydroxyimidazoacridinone  
62 (C-1311) (Fig. 1) has received significant attention due to its exceptionally high cytotoxic  
63 activity against a broad spectrum of human tumor cell lines in the National Cancer Institute *in*  
64 *vitro* screening system and of transplantable animal tumors [2,3]. This compound reached up  
65 the phase II clinical trials where exhibited activity against advanced solid tumors, and it was  
66 effective in women with metastatic breast cancer [4]. Furthermore, it turned out to be an agent  
67 with high-predicted activity in human bladder cancer [5].

68 The leading concept to find out how C-1311 causes high antitumor effect is the metabolic  
69 (oxidative and/or reductive) activation of the compound to species responsible for cell injury  
70 and death. It was demonstrated [6] that intercalation of C-1311 into DNA followed by its  
71 activation under enzymatic oxidative conditions gave rise to products capable of irreversible  
72 binding into DNA. Therefore, the knowledge about the route of metabolism of the drug  
73 candidate was desirable to determine its pharmacological and/or toxicological activity. Multiple  
74 studies on the molecular mechanism of the enzymatic activation of C-1311 with different liver  
75 drug-metabolizing enzymes were performed [7-10]. Various cytochrome P450 (P450) isoforms  
76 are among the many intracellular enzymes that catalyze activation reactions. Specifically,  
77 P450 enzymes are responsible for the biotransformation of about 70-80% of all drugs in clinical  
78 use [11]. However, no products of C-1311 metabolism were observed with any tested human  
79 recombinant P450s [8]. In contrast, C-1311 has been identified as a potent mechanism-based  
80 inactivator of P450 1A2 and 3A4 isoenzymes [9]. On the other hand, C-1311 was a good  
81 substrate for microsomal and the selected human recombinant flavin-containing  
82 monooxygenases and UDP-glucuronosyltransferases [8,10]. The knowledge on the biological  
83 background of C-1311 metabolism and its influence on human body is constantly increasing,  
84 but still molecular mechanisms have not been completely explained.

85 Drug metabolism studies are an integral part of the comprehensive characterization of a  
86 new chemical entity during various stages of the drug development process. In order to



87 address this challenging task, different methods for the simulation of metabolic reactions have  
88 been developed and applied. In practice, the studies on drug metabolism usually include *in*  
89 *vivo* experiments on the basis of animal models, or *in vitro* tests, where P450-containing  
90 matrices like hepatocytes, liver microsomes, and other cellular fractions derived from animal  
91 or human tissue are used [12] (Fig. 2A). Although the biological systems are still being  
92 improved, there are a number of drawbacks associated with these approaches (e.g., the great  
93 expense of biological material and cofactors, the ethical aspect of using biological material of  
94 human or animal origin). From a practical aspect, both *in vitro* and *in vivo* systems inherently  
95 have a complex biological matrix that makes isolation and purification of metabolites time-  
96 consuming and laborious [13]. Therefore, analytical techniques which are able to mimic  
97 metabolic reactions taking place in the human body and which simultaneously allow to reduce  
98 the listed above limitations, gain strong attention.

99 In recent years a particular interest in the field of drug metabolism studies has been  
100 observed from electrochemistry. Complementary to the existing techniques, oxidation-  
101 reduction reactions catalyzed by liver P450 isoforms can be successfully simulated in an  
102 electrochemical (EC) cell coupled directly to a mass spectrometer (MS) [14,15]. This simple  
103 and pure instrumental technique allows for the generation of a number of potential oxidative  
104 metabolites, including reactive intermediates, and for the detection of the sites labile towards  
105 oxidation in a drug molecule [16,17]. The greatest advantage of the electrochemical studies on  
106 oxidative metabolic reactions over other *in vitro* methods is the absence of proteins in the  
107 reaction medium. Moreover, in EC system it is possible to control the reaction rate by the  
108 applications of electrode potentials specific for synthesis of the expected products [15].

109 Considering the mechanistic differences between EC and enzymatic oxidations, not all  
110 metabolic pathways can be mimicked by EC. Thus, EC cannot replace conventional  
111 metabolism studies in biological systems. However, this technique may serve as an attractive  
112 alternative tool for the initial investigation of drug metabolism in a single-step experiment. In  
113 this work, we explored the on-line combination of EC with electrospray ionization (ESI) MS for  
114 metabolism studies of antitumor drug candidate C-1311 (Fig. 2B). The main focus of the



115 present study was to put on the simulation of potential oxidation transformations of the  
116 compound with the prediction of metabolite structures by the identification of sites susceptible  
117 to oxidation. Further, the obtained results were supported by *in silico* computational method  
118 (Fig. 2C). It is usually a starting point of metabolic pathway studies, which may also assist in  
119 the process of drug/lead optimization [18]. MetaSite software, applied in this study, considered  
120 the enzyme-substrate recognition and the chemical transformations induced by the P450  
121 enzymes on the most reactive sites. It attributed the more probable sites of metabolism, and  
122 therefore predicted the main metabolites that can be formed in various human tissues (liver,  
123 skin, brain, and lungs) [19]. Our choice of two major human P450s: 1A2 and 3A4 resulted from  
124 our earlier findings revealing that these P450 isoenzymes were irreversible inhibited by the  
125 studied imidazoacridinone, probably according to mechanism-based manner [9]. However, no  
126 reactive intermediate products, which would be responsible for autoinactivation of P450  
127 enzymes, have been detected so far. In turn, P450 2D6 isoform was taken into account due to  
128 its specific involvement in aliphatic and aromatic hydroxylations [20]. In order to obtain insight  
129 into the potential of EC for the simulation of drug metabolism, the results of EC/MS analyses  
130 were also referred to the data of previous *in vitro* experiments on C-1311 in the presence of  
131 rat and human liver microsomes [7] and in the model activation system, horseradish  
132 peroxidase/hydrogen peroxide [21]. An overview of the compared approaches used in drug  
133 metabolism studies was shown in Fig. 2.

134 The comparison and correlation of the results obtained in various systems for drug  
135 metabolism studies are important for better understanding of C-1311 metabolic pathways.  
136 Conventional enzymatic approaches remain methods of choice for determination of phase I of  
137 drug metabolism. In turn, EC and *in silico* methods, that enable determinations of metabolism  
138 patterns, may be considered as fast alternatives to *in vitro* schemes, even though the results  
139 are not unrestrictedly transferable to the situation in the human liver. Further, structural  
140 characterization of metabolites allows the modification of drug molecule to decrease the  
141 metabolic clearance or to avoid unwanted metabolic transformations, what may contribute to  
142 the development of new derivatives with improved metabolic properties [14,22].



## 143 **2. Materials and methods**

### 144 **2.1. Chemicals**

145 Imidazoacridinone derivative, a 5-diethylaminoethylamino-8-hydroxyimidazoacridinone  
146 (C-1311) was synthesized and purified in our laboratory according to the method described  
147 earlier [1]. Formic acid (FA) was purchased from Sigma-Aldrich (St. Louis, MO, USA).  
148 Ammonium formate ( $\text{NH}_4\text{HCO}_2$ ) was ordered from Fisher Scientific (Loughborough, UK).  
149 Methanol (MeOH) and acetonitrile (ACN) (both in gradient grade quality for liquid  
150 chromatography) were obtained from Merck KGaA (Darmstadt, Germany). All other  
151 commercially available chemicals and reagents were of the highest possible grade available.  
152 Ultrapure water (conductivity 18.2 M $\Omega$  cm), used in all the experiments, was passed through a  
153 Milli-Q water purification system from Merck KGaA.

### 154 **2.2. General instrumentation**

#### 155 **2.2.1. Electrochemistry (EC)**

156 The EC system used for electrochemical experiments simulating P450-mediated oxidative  
157 reactions was set up as reported in previous investigations [23]. The ROXY™ potentiostat was  
158 equipped with a commercial electrochemical thin-layer ReactorCell™ and a SP2-ROXY™  
159 Dual-Piston Syringe Pump (Antec Leyden, Zoeterwoude, The Netherlands). A three-electrode  
160 configuration was used in the present study, *i.e.*, a disc glassy carbon working electrode ( $\phi =$   
161 8 mm;  $A = 0.502 \text{ cm}^2$ ), the HyREF™ palladium-hydrogen (Pd/H<sub>2</sub>) reference electrode, and the  
162 carbon-loaded PTFE (polytetrafluoroethylene) auxiliary electrode. Representative results of at  
163 least three independent experiments were considered. The glassy carbon working electrode  
164 surface was wiping with a tissue wetted with methanol and/or was finished with a polishing  
165 disc and diamond slurry provided by the manufacturer (Antec Leyden) prior to each  
166 experiment.

#### 167 **2.2.2. Mass spectrometry (MS)**

168 For the generation of two-dimensional (2-D) mass voltammograms, the outlet of the ROXY™  
169 EC system was directly connected to the standard ESI source of an Agilent 6500 Series  
170 Accurate-Mass Quadrupole-Time of Flight (Q-TOF) mass spectrometer (Agilent Technologies,



171 Santa Clara, CA, USA) by means of 50 cm long PEEK tubing (130  $\mu\text{m}$  I.D.). The system was  
172 controlled by Agilent MassHunter Workstation software (Agilent Technologies). The scan  
173 range was set from 50 to 600 mass-to-charge ratio ( $m/z$ ) and mass spectrometric detection  
174 was carried out in the positive ionization mode (+). Tandem mass spectrometry (MS/MS) mode  
175 was used to provide additional structural information for the ions of interest. To ensure accurate  
176 mass during the experiment, the mass spectrometer was calibrated daily using calibration  
177 solution (ES-TOF reference mix, Agilent Technologies). The corresponding conditions for the  
178 ESI-Q-TOF-MS measurements and the optimized parameters for the ESI-ion trap MS/MS  
179 experiments can be viewed in Table 1.

180 The delay time between product formation within the EC cell and detection in the MS was  
181 taken into account. It was calculated on the basis of the dead volume between the reactor cell  
182 and the ion source of the MS (for the supplied tubing this volume was 12.7  $\mu\text{L}$ ) and the flow  
183 rate of the infusion syringe pump (30  $\mu\text{L min}^{-1}$ ). The transfer time to the capillary was estimated  
184 at about 0.7 min. Therefore, the oxidation behavior of C-1311 was observed in real time during  
185 application of a potential ramp to the EC cell.

### 186 **2.2.3. Liquid chromatography (LC)**

187 The mixture of C-1311 and its putative oxidation products leaving the EC cell was also  
188 collected and analysed by LC/MS. Liquid chromatographic separations were performed on a  
189 reversed-phase (RP) 5- $\mu\text{m}$  Suplex pKb-100 analytical column (4.6 mm x 250 mm, C18)  
190 (Supelco Inc., Bellefonte, PA, USA) with Agilent 6500 Series Accurate-Mass Q-TOF LC/MS  
191 system (Agilent Technologies) controlled by Agilent MassHunter Workstation software. The  
192 mobile phase consisted of 0.05 M aqueous  $\text{NH}_4\text{HCO}_2$  buffer (pH 3.4 adjusted with FA; solvent  
193 A) and MeOH (solvent B). The LC analyses were carried out at a flow rate of 1  $\text{mL min}^{-1}$  with  
194 the following mobile phase system: a linear gradient from 15% to 80% B in A for 25 min,  
195 followed by a linear gradient from 80% to 100% B in A for 3 min, and 2 min isocratic 100% B.  
196 During all LC separations, the column was operated at a room temperature. The eluates were  
197 monitored at 380 nm. The MS conditions were identical to those described above.

### 198 **2.3. Electrochemical simulation of the oxidative metabolism of C-1311**



199 A stock solution of C-1311 was prepared in an electrolyte (composition described below) at a  
200 concentration of 1 mg mL<sup>-1</sup>. It was used to prepare fresh working solutions of C-1311 (0.01 mg  
201 mL<sup>-1</sup>) shortly before each experiment. Two electrolytes of different pH values were used for  
202 optimization of the electrochemical conditions: (1) H<sub>2</sub>O-MeOH (1:1, v/v) with 0.1% FA, pH 3.3;  
203 (2) 20 mM NH<sub>4</sub>HCO<sub>2</sub>-ACN (1:1, v/v), pH 7.4. Simulation of the oxidative phase I metabolism of  
204 C-1311 in the EC cell was accomplished at a constant flow rate of 30 μL min<sup>-1</sup>. The potential  
205 of the working electrode was ramped linearly from 0 V up to 2.5 V at 10 mV s<sup>-1</sup> and was  
206 controlled by the Dialogue software (Antec Leyden). The relevant EC conditions are listed in  
207 Table 1. The outlet of the reactor cell was connected on-line to the ESI-MS source.

#### 208 **2.4. *In silico* prediction of cytochrome P450-mediated sites of C-1311 metabolism**

209 The MetaSite software tool (version 5.1.1; Molecular Discovery Ltd., Hertfordshire, UK) is a  
210 computational algorithm used to identify most likely metabolic soft-spots of xenobiotics. The  
211 software considers two factors: chemical reactivity of the substrate and structural  
212 complementarity between the active site of the P450 enzyme and the ligand and comes up  
213 with the most optimal orientation [24]. A 2-D structure of the C-1311 was imported into the  
214 interface of MetaSite to predict phase I sites of metabolism and structures of metabolites in  
215 liver related to P450 1A2-, 3A4-, and 2D6-mediated reactions. Only metabolites with a  
216 molecular mass higher than 150 Da and with a likelihood ranking >50% were considered.

### 217 **3. Results and discussion**

218 The main focus of this study was directed to the combination and comparison of *in vitro* and *in*  
219 *silico* approaches for the determination of C-1311 metabolism. First, the oxidation of C-1311  
220 in an electrochemical thin-layer cell was employed for fast and easy generation of the possible  
221 phase I metabolites. Then, *in silico* prediction of the sites of C-1311 biotransformation mediated  
222 by cytochromes P450 using the MetaSite software tool was carried out to support the  
223 experimental data found via EC. The results deriving from both the EC and *in silico* studies  
224 were also compared with those of the most common *in vitro* investigations with rat and human  
225 liver microsomes and in the model peroxidase system, which were discussed in detail  
226 elsewhere [7,21].

#### 227 **3.1. Electrochemical simulation of C-1311 oxidative metabolism**

228 The determination of the metabolic fate of drugs is an essential and important part of the drug  
229 development process. Progress in this research area depends critically on the improvement of  
230 methods involved in the generation and analysis of various types of drug metabolites. In the  
231 current study, the on-line coupling of EC with ESI-MS (Fig. 2B) is an effective analytical tool  
232 for the studies on the oxidation products of antitumor-active compounds developed in our  
233 laboratory, since experiments are done under controlled conditions using pure solvents and  
234 reagents. Additionally, the absence of the components of biological matrices in the  
235 electrochemical reaction medium, prevents the further laborious tasks related to isolation and  
236 identification of metabolic products formed in conventional enzymatic systems. Consequently,  
237 data analysis process is accelerated [25].

##### 238 **3.1.1. Optimization of the electrochemical conditions**

239 The optimization of the electrochemical conditions is of great importance for a successful  
240 comparison with conventional *in vitro* enzymatic approaches. The conversion efficiency in the  
241 EC cell may be influenced by the properties of the sample solvent. Therefore, the  
242 electrochemical simulation of the oxidative metabolism of C-1311 has been performed in two  
243 electrolyte solutions with different composition and pH value (see Materials and methods  
244 section). The flow rate of the sample solution through the reactor cell and the potential applied



245 at a working electrode may also affect the EC efficiency. All these parameters were optimized  
246 for the best conditions for oxidation and identification processes. In result, the most effective  
247 conversion of C-1311 into its expected metabolites was attained with use of the H<sub>2</sub>O-MeOH  
248 (1:1, v/v) with 0.1% FA electrolyte (pH 3.3) and glassy carbon as a working electrode material  
249 for voltage range between 0 and 2.5 V. Additionally, we have observed that methanol was  
250 better than acetonitrile in diminishing the adsorption of the electrochemical products on the  
251 surface of the working electrode what resulted in greater signal intensity of the selected mass  
252 ions. Moreover, H<sub>2</sub>O-MeOH electrolyte solution produced the lowest mass background noise  
253 in positive total ion chromatograph (data not shown). Details regarding the optimized EC  
254 conditions used for measurements can be found in Table 1.

### 255 **3.1.2. On-line EC/MS experiments**

256 Initially, a solution of C-1311 was directly introduced from the syringe pump into the EC cell  
257 without applying a voltage to the working electrode (cell off). Due to the presence of the  
258 nitrogen atoms in the side chain, the C-1311 molecule can easily be protonated and detected  
259 with high intensities as [M+H]<sup>+</sup> ion (*m/z* 351.1820) (Fig. 3A) in the positive ionization mode of  
260 the ESI-Q-TOF mass spectrometer. In turn, applying a voltage to the EC cell (cell on) led to C-  
261 1311 oxidation and resulted in a reduction in ion signal corresponding to the substrate.  
262 Simultaneously, oxidation products of C-1311 were formed and new signals of the [M+H]<sup>+</sup> ions  
263 corresponding to putative oxidation products were observed (Fig. 3B). To provide a concise  
264 overview of the oxidation products, 2-D mass voltammograms for the ions of interest were  
265 generated (Fig. 4) by plotting the intensities of the extracted ions against time of  
266 electrochemical analysis. A total of eight putative products of C-1311 were generated by EC.  
267 The electrosynthesis of various products required operation at different potential settings. The  
268 vast majority of products were generated at potentials between 1 and 2 V, and to form the  
269 products at *m/z* 365 and *m/z* 367 the higher values of potentials were required.

### 270 **3.1.3. Characterization of the products**



271 Combining EC system on-line with MS allowed the initial characterization of the formed  
272 products by an increasing signal intensity of the corresponding  $m/z$ . Their molecular structures  
273 have been derived based on calculations with accurate mass data (mass  
274  $\leq 2$  ppm). The fragmentation (MS/MS) spectra were also recorded. In turn, the separation of  
275 oxidation products by reversed-phase LC can overcome ion suppression effects that may be  
276 encountered during on-line EC/MS thus providing additional information about the range of  
277 oxidation products and, consequently, about the reaction mechanism [26]. However, unstable  
278 products may escape analysis. Therefore, both approaches (EC/MS and LC/MS) were  
279 employed for a comprehensive analysis. LC method was established based on the preliminary  
280 results from 2-D mass voltammograms. Extracted ion chromatograms of C-1311 and its  
281 products that were generated electrochemically are presented in Fig. 5.

282 A comprehensive summary of the products detected following oxidative transformation of  
283 C-1311 in the EC cell was shown in Table 2. *N*-Dealkylation is a characteristic type of *in vitro*  
284 and *in vivo* metabolic transformation catalyzed by cytochrome P450 enzymes and it is a major  
285 metabolism pathway for drugs containing secondary and tertiary amines [27]. This process  
286 can also be easily induced electrochemically [14,15,28]. A signal at  $m/z$  252 (P1) involves a  
287 reduction in mass by 99 Da what can be explained by a loss of diethylaminoethyl moiety as a  
288 result of complete *N*-dealkylation in the side chain of C-1311 molecule. In turn, the P3 product  
289 ( $m/z$  323; - 28 Da) may arise from an *N*-deethylation reaction. Postulated mechanism of the  
290 electrochemical *N*-dealkylation of *N*-alkylamines proceeds through one-electron transfer to  
291 generate an imine intermediate that, after hydrolysis and intramolecular rearrangement, gives  
292 the product of *N*-dealkylation [27]. For further confirmation of the *N*-dealkylated derivatives, the  
293 fragmentation patterns, generated by in-source fragmentation in the ESI interface, have been  
294 studied. The Q-TOF-MS/MS spectrum obtained for  $m/z$  323 ion (Fig. 6A) showed fragment  
295 ions at  $m/z$  252 (- 99 Da) and  $m/z$  278 (- 73 Da). While the former can be assigned to the *N*-  
296 dealkylation process, the latter can indicate an intermediate product of a side chain  
297 degradation (P2) that was also detected in the EC system. In the elution profile (according to  
298 gradient profile used for LC analysis) the P1 peak was eluted at 20.47 min (Fig. 5) so that it



299 appeared after the peak corresponding to the mass ion at  $m/z$  351 (C-1311;  $t_R$  14.33 min).  
300 Hence, it would indicate its less polar nature than that of the substrate. P3 product was found  
301 in trace amounts in LC analysis.

302 Dealkylation is usually considered as an element of the detoxification pathway of  
303 xenobiotics [27]. In this sense, the metabolic transformation leading to the *N*-dealkylated  
304 products should give probably the less toxic, inactive metabolites. Both *N*-dealkylated  
305 products, P1 and P3, were also observed in horseradish peroxidase/hydrogen peroxide  
306 system [21], while only the product P3 was detected in similar amounts after incubation with  
307 rat and human microsomes [7]. Consequently, the presented electrochemical reactor seems  
308 to be better suited for simulating the P450-catalyzed *N*-dealkylation reactions than liver  
309 microsomes. This may be related to the fact that, although liver microsomes contain the  
310 physiologically relevant combinations of drug-metabolizing enzymes, expression of different  
311 P450 isoforms may be very diverse in the organism. On the other hand, primary amines are  
312 the most common quasi-irreversible P450 inactivators [29]. The resulting primary amine may  
313 be further oxidized to nitroso derivative (via the intermediate hydroxylamine metabolite), which  
314 can form a metabolic intermediate complex with the ferrous form of the heme iron atom.  
315 Therefore, secondary and tertiary amines can serve as suitable precursors for enzyme  
316 inactivation provided they are *N*-dealkylated to primary amines. This is in agreement with the  
317 previous knowledge on the metabolic activation of C-1311 [9].

318 The dehydrogenation reaction is a special feature of P450 in which it actually behaves as  
319 an oxidase-dehydrogenase, and converts molecular oxygen to water [27]. In addition to *N*-  
320 dealkylation, dehydrogenation can also be imitated by direct electrochemical oxidation where  
321 it is proposed to undergo through two successive electron/proton transfer reactions [14,15].  
322 The obtained mass ion at  $m/z$  349 correlates with the loss of two hydrogen atoms (- 2 Da) what  
323 indicates the generation of the dehydrogenated product (P4). To elucidate the nature of this  
324 compound, the LC/MS analysis was performed. The peak at  $m/z$  349 (Fig. 5) was eluted ahead  
325 of C-1311 at 11.88 min what suggests rather higher hydrophilicity of the respective compound  
326 than that of the substrate. It is assumed that a carbon-carbon double bond is formed in the



327 side chain what is energetically advantageous because provides an extra stability due to the  
328 possibility of resonance with the electrons of the aromatic system. Electrochemical  
329 dehydrogenation of a carbon-carbon bond has been observed for a number of drug  
330 compounds [14,28,30].

331 Electrochemical conversion of C-1311 mainly led to the formation of the products P5 and  
332 P6, resulting in the signals at  $m/z$  365 and  $m/z$  367, respectively (Fig.4B). In the case of the  
333 first one, an increase in mass by 14 Da, compared with  $m/z$  351 (C-1311), can be explained  
334 by a two-step process, consisting of oxidation (+ O), followed by the dehydrogenation (- 2H).  
335 This may indicate a route leading to an aldehyde or a ketone. The second mass ion suggests  
336 the introduction of one oxygen atom into the C-1311 molecule, shown by a mass increase of  
337 16 Da. The insertion of an oxygen atom may take place under the formation of a hydroxyl  
338 group (aromatic or aliphatic hydroxylation) or by *N*-oxidation. Carbon hydroxylation is a very  
339 common P450-catalyzed reaction [27] and the utility of electrochemistry for simulation of this  
340 process for pharmaceutical drugs and xenobiotics is well documented [14,16,17]. The LC  
341 separation of the electrochemically generated products revealed that two different isomers  
342 (peaks P6a and P6b in Fig. 5) of a species with  $m/z$  367, showing similar intensities, could be  
343 detected. Their retention times of 14.79 min and 16.22 min, respectively, were higher than C-  
344 1311 what confirmed the assumption that the hydroxylated products might have been formed.  
345 Moreover, these peaks may be attributable to hydroxylation on different sites of the C-1311  
346 molecule.

347 MS/MS spectrum of  $m/z$  367 showed the fragment ions at  $m/z$  350 and the most abundant  
348  $m/z$  336 (Fig. 6C). The existence of fragment ion at  $m/z$  350 may indicate the loss of one  
349 hydroxyl group (- 17 Da), what can hardly be in agreement with an *N*-oxide structure, while the  
350 latter may arise from the heterolytic beta cleavage of carbon-carbon bond that released a  
351 CH<sub>2</sub>OH molecule (- 31 Da). Hence, one of the isomers of the P6 product may be associated  
352 with a singly hydroxylated species bearing the additional oxygen atom at the terminal carbon  
353 atom ( $\omega$  position) of the ethyl group of the nitrogen atom. In this study, working at higher  
354 potentials enabled aliphatic carbon to be hydroxylated. According to previous studies on C-



355 1311 metabolism [7,8,21], the likely hydroxylation site in the C-1311 molecule may also be the  
356 imidazoacridinone moiety. However, no evidence was found for the formation of an aromatic  
357 alcohol and our findings strongly show that hydroxylation on the side chain of the compound  
358 appears to be more preferential in electrochemistry. On the other hand, *N*-oxidation could not  
359 be excluded, since the product at *m/z* 367 was obtained in both rat as well as human liver  
360 microsomes [7] and in metabolism of C-1311 with FMO [8], and have been proposed to be *N*-  
361 oxide derivative on the  $\omega$ -nitrogen atom of C-1311. The peak of the 6a isomer, with a slightly  
362 higher retention time than C-1311, may just point out the presence such a product.  
363 Interestingly, the identical fragment ion at *m/z* 336 was also seen in MS/MS spectrum of *m/z*  
364 365 (Fig. 6B). This time it is implied that the loss of COH molecule took place what confirms  
365 the further oxidation of the P6 to the corresponding aldehyde.

366 The next oxidation products P7 and P8 exhibited strong signals at *m/z* 379 and *m/z* 381,  
367 respectively. Despite showing quite good intensities in the EC/MS system, both products were  
368 not found in LC/MS analysis and no MS/MS data were accessible for them. This may be due  
369 to the limited stability of these reaction products. Thus, the assigned structures of P7 and P8  
370 are to be regarded as tentative. The determined exact mass of *m/z* 379.1764 indicates the  
371 formation of a derivative with an additional formyl group (-CHO; calculated: *m/z* 379.1764,  
372 mass error 0.0 ppm) rather than a product of double oxidation (+ 2O, - 4H; calculated: *m/z*  
373 379.1401, mass error 95.8 ppm). It presumably occurred through the reaction of C-1311 with  
374 formic acid present in the electrolyte solution. In turn, the P8 product is proposed to be the P7  
375 corresponding alcohol. A general overview of the proposed pathways of C-1311  
376 electrochemical oxidation is shown in Fig. 7.

### 377 **3.2. *In silico* prediction of cytochrome P450-mediated sites of C-1311 metabolism**

378 No stable final products of C-1311 metabolism with P450 isoenzymes have been observed  
379 so far [8], but the results of cytochrome P450 1A2 and 3A4-inhibitory activities of the compound  
380 [9] strongly suggest the possibility of any metabolic activation pathway. C-1311, as a prodrug,  
381 could be also activated by the action of P450 2D6 that is an isoenzyme specifically involved in  
382 aliphatic and aromatic hydroxylations [20]. Our former studies and these presented above



383 pointed that the most reactive site in the C-1311 molecule was expected to be diethylamino  
384 functional group. In this study, for the demonstration of the suitability of the electrochemical  
385 system in drug metabolism studies, prediction of C-1311 metabolism was performed with the  
386 use of MetaSite 5.1.1 software tool (Molecular Discovery Ltd.). The results of the proposed the  
387 most probable metabolites with their molecular weight and calculated cLogP (the logarithm of  
388 the partition coefficient between *n*-octanol and water) are presented in Table 3.

389 Five and six top ranked phase I metabolite structures were predicted in the case of  
390 P450 1A2 and 3A4 isoforms, respectively. The dialkylaminoalkylamino moiety was proved to  
391 be the most probable site of P450 attack in the C-1311 molecule. In both cases, the *N*-  
392 deethylation products were obtained (MW 322.14; 50% and 100% of likelihood for P450 1A2  
393 and 3A4, respectively), wherein complete *N*-dealkylation (MW 251.07; 100% of likelihood) is  
394 likely only with the participation of P450 1A2 isoenzyme. MetaSite also indicated the possibility  
395 of hydroxylation (MW 366.17; 100% of likelihood for P450 1A2) and oxidation (MW 364.15) on  
396 various positions of the side chain but with the indication of the  $\omega - 1$  carbon atom of the  
397 terminal ethylamino group as preferential (50% and 100% of likelihood for P450 1A2 and 3A4,  
398 respectively). The most likely metabolite for P450 1A2 activity was also formed by oxidative  
399 deamination and the following oxidation on the imidazoacridinone ring (MW 266.03; 100% of  
400 likelihood). This electrophilic *ortho*-quinone derivative may potentially be implicated in the  
401 covalent apoprotein modification of P450 isoenzymes. Hence, its existence may be associated  
402 with the observed stronger inactivation of P450 1A2 than 3A4 by C-1311 [9]. Probably due to  
403 its high chemical reactivity, this product was not detected in the EC/MS system. Oxidative  
404 deamination product (MW 293.08) and its corresponding carboxylic acid (MW 309.07), both  
405 with an equal likelihood of 50%, were predicted in the case of P450 3A4. Another main  
406 metabolite of this P450 isoenzyme was that derived by dehydrogenation in the ethylamino  
407 chain (MW 348.16; 50% of likelihood). Considering P450 2D6-mediated sites of C-1311  
408 metabolism, MetaSite predicted the *ortho* position to the hydroxyl group in the acridinone  
409 moiety as the most probable site of C-1311 hydroxylation (MW 366.17; 100% of likelihood).  
410 The resulting diol derivative may contribute to overall cytotoxic activity of the compound



411 because it is a preferred structure for the substitution by nucleophiles existing in a living  
412 organism (*i.e.*, glutathione, thiols of proteins or purine and pyrimidine bases of DNA). However,  
413 the predicted hydroxylation would take place also in the aliphatic chain giving a compound with  
414 the identical MW of 366.17 but with 50% of likelihood. These structures are the result of  
415 hydroxylation reactions typical for P450 2D6 catalytic activity. Two other products provided by  
416 MetaSite, with the same 50% of likelihood, were identical with those indicated for P450 1A2  
417 (*N*-deethylated product) and 3A4 (dehydrogenated product), whereas the structure of the  
418 oxygenated product (MW 364.15; 50% of likelihood) was different.

419 In case of all predicted metabolites the calculated cLogP values were in the range of -1.56  
420 to 2.67 (for P450 1A2), 1.56 to 2.52 (for P450 3A4), and 1.21 to 2.62 (for P450 2D6). It means  
421 that they are rather more hydrophilic substances compared to the parent compound (cLogP  
422 2.78). This is with accordance with general rule that metabolism of chemicals generates polar  
423 water-soluble metabolites what causes their poorer absorption or permeation in biological  
424 systems but improves excretion from the body.

425 Summing up, MetaSite-based *in silico* predictions for sites of C-1311 metabolism  
426 supported electrochemical findings. MetaSite correctly predicted the identical *N*-dealkylation  
427 and dehydrogenation products generated in the EC system. A number of hydroxylation and  
428 oxidation products were also predicted by *in silico* analysis. However, we found that there are  
429 some discrepancies in the sites of hydroxylation or oxidation between *in silico* and  
430 electrochemical predictions. Firstly, the formation of different isomers cannot be observed from  
431 direct on-line EC/MS(/MS), as they often show similar fragmentation patterns in tandem MS.  
432 To obtain the stereochemistry induced by different P450 isoenzymes, it would be necessary  
433 to modify the electrode surfaces. Secondly, EC yields products resulting from the most labile  
434 sites in a molecule sensitive to oxidation or reduction. *In silico* system is based on the  
435 prediction of enzyme-substrate interactions (specific to individual P450 isoform), where, in  
436 contrast to the EC method, the regioselectivity of drug oxidation is often governed by the  
437 topology of the active site of P450's [14,16,17]. Table 4 represents a quick overview of all



438 oxidative products of C-1311 detected by application of various methods for metabolism  
439 studies.

#### 440 4. Conclusions

441 The present work is a clear demonstration of the usefulness of electrochemistry connected on-  
442 line to mass spectrometry for the drug metabolism studies. Electrochemical conversion of the  
443 studied antitumor imidazoacridinone C-1311 resulted in the products of *N*-dealkylation,  
444 dehydrogenation, hydroxylation and oxidation reactions what confirmed that the cytochrome  
445 P450-mediated metabolism of pharmaceuticals can be efficiently simulated in an  
446 electrochemical cell. The foregoing experiments revealed that some of the products generated  
447 electrochemically were in a good agreement with those predicted by *in silico* analysis and those  
448 previously reported from *in vitro* enzymatic incubations. Furthermore, electrochemical method  
449 was also found to provide unique features not identified with other approaches. The observed  
450 discrepancies between EC- and P450-generated metabolites may be due to the mechanistic  
451 differences between EC and enzymatic oxidations or may result from the efficiency of a given  
452 method. Nonetheless, electrochemically-mediated transformations supported with *in silico*  
453 methods can be considered as a convenient and simple alternative to *in vitro* enzymatic  
454 assays. The simplicity of the EC system, and the ease and speed with applying to a large  
455 number of compounds, make it a useful tool for the initial investigation of drug metabolism.

456 **Conflicts of interest**

457 There are no conflicts to declare.

458

459 **Acknowledgements**

460 The authors thank Professor Agata Kot-Wasik (Department of Analytical Chemistry, Faculty of  
461 Chemistry, Gdańsk University of Technology, Poland) for cooperation in the field of MS(/MS)  
462 analysis.

463

464 **Funding**

465 This work was supported by the National Science Center, Poland [the grant number  
466 2012/07/D/NZ7/03395].

467 **References**

- 468 [1] W. M. Cholody, S. Martelli, J. Paradziej-Lukowicz, J. Konopa, 5-  
469 [(Aminoalkyl)amino]imidazo[4,5,1-de]acridin-6-ones as a novel class of antineoplastic  
470 agents. Synthesis and biological activity, *J. Med. Chem.* 33 (1990a) 49-52.
- 471 [2] B. Berger, H. Marquardt, J. Westendorf, Pharmacological and toxicological aspects of new  
472 imidazoacridinone antitumor agents, *Cancer Res.* 56 (1996) 2094-2104.
- 473 [3] A. M. Burger, J. A. Double, J. Konopa, M. C. Bibby, Preclinical evaluation of novel  
474 imidazoacridinone derivatives with potent activity against experimental colorectal cancer,  
475 *Br. J. Cancer* 74 (1996) 1369-1374.
- 476 [4] N. Isambert, M. Campone, E. Bourbouloux, M. Drouin, A. Major, W. Yin, P. Loadman, R.  
477 Capizzi, C. Grieshaber, P. Fumoleau, Evaluation of the safety of C-1311 (SYMADEX)  
478 administered in a phase I dose-escalation trial as a weekly infusion for 3 consecutive weeks  
479 in patients with advanced solid tumors, *Eur. J. Cancer* 46 (2010) 729-734.
- 480 [5] S. C. Smith, D. M. Havaleshko, K. Moon, A. S. Baras, J. Lee, S. Bekiranov, D. J. Burke, D.  
481 Theodorescu, Use of yeast chemigenomics and COXEN informatics in preclinical  
482 evaluation of anticancer agents, *Neoplasia* 13 (2011) 72-80.
- 483 [6] Z. Mazerska, J. Dziegielewski, J. Konopa, Enzymatic activation of a new antitumour drug,  
484 5-diethylaminoethylamino-8-hydroxyimidazoacridinone, C-1311, observed after its  
485 intercalation into DNA, *Biochem. Pharmacol.* 61 (2001) 685-694.
- 486 [7] A. Wiśniewska, A. Chrapkowska, A. Kot-Wasik, J. Konopa, Z. Mazerska, Metabolic  
487 transformations of antitumor imidazoacridinone, C-1311, with microsomal fractions of rat  
488 and human liver, *Acta Biochim. Pol.* 54 (2007) 831-838.
- 489 [8] A. Potęga, E. Dabrowska, M. Niemira, A. Kot-Wasik, S. Ronseaux, J. C. Henderson, C. R.  
490 Wolf, Z. Mazerska, The imidazoacridinone antitumor drug, C-1311, is metabolized by  
491 FMOs but not cytochrome P450s, *Drug Metab. Dispos.* 39 (2011) 1423-1432.
- 492 [9] A. Potęga, B. Fedejko-Kap, Z. Mazerska, Imidazoacridinone antitumor agent C-1311 as a  
493 selective mechanism-based inactivator of human cytochrome P450 1A2 and 3A4  
494 isoenzymes, *Pharmacol. Rep.* 68 (2016) 663-670.



- 495 [10] B. Fedejko-Kap, S. M. Bratton, M. Finel, A. Radomska-Pandya, Z. Mazerska, Role of  
496 human UDP-glucuronosyltransferases in the biotransformation of the triazoloacridinone  
497 and imidazoacridinone antitumor agents C-1305 and C-1311: highly selective substrates  
498 for UGT1A10, *Drug Metab. Dispos.* 40 (2012) 1736-1743.
- 499 [11] U. M. Zanger, M. Schwab, Cytochrome P450 enzymes in drug metabolism: Regulation of  
500 gene expression, enzyme activities, and impact of genetic variation, *Pharmacol. Ther.* 138  
501 (2013) 103-141.
- 502 [12] S. Asha, M. Vidyavathi, Role of human liver microsomes in in vitro metabolism of drugs -  
503 a review, *Appl. Biochem. Biotechnol.* 160 (2010) 1699-1722.
- 504 [13] E. F. Brandon, C. D. Raap, I. Meijerman, J. H. Beijnen, J. H. Schellens, An update on in  
505 vitro test methods in human hepatic drug biotransformation research: pros and cons,  
506 *Toxicol. Appl. Pharmacol.* 189 (2003) 233-246.
- 507 [14] U. Jurva, H. V. Wikstrom, L. Weidolf, A. P. Bruins, Comparison between  
508 electrochemistry/mass spectrometry and cytochrome P450 catalyzed oxidation reactions,  
509 *Rapid Commun. Mass Spectrom.* 17 (2003) 800-810.
- 510 [15] E. Nouri-Nigjeh, R. Bischoff, A. P. Bruins, H. P. Permentier, Electrochemistry in the mimicry  
511 of oxidative drug metabolism by cytochrome P450s, *Curr. Drug Metab.* 12 (2011) 359-371.
- 512 [16] U. Bussy, M. Boujtita, Advances in the electrochemical simulation of oxidation reactions  
513 mediated by cytochrome P450, *Chem. Res. Toxicol.* 27 (2014) 1652-1668.
- 514 [17] A. Baumann, U. Karst, Online electrochemistry/mass spectrometry in drug metabolism  
515 studies: principles and applications, *Expert Opin. Drug Metab. Toxicol.* 6 (2010) 715-731.
- 516 [18] M. Zheng, X. Luo, Q. Shen, Y. Wang, Y. Du, W. Zhu, H. Jiang, Site of metabolism prediction  
517 for six biotransformations mediated by cytochromes P450, *Bioinformatics* 25 (2009) 1251-  
518 1258.
- 519 [19] A. Tarcsay, G. M. Keseru, In silico site of metabolism prediction of cytochrome P450-  
520 mediated biotransformations, *Expert Opin. Drug Metab. Toxicol.* 7 (2011) 299-312.



- 521 [20] P. R. Ortiz De Montellano, J. J. De Voss, Substrate oxidation by cytochrome P450  
522 enzymes, in: P. R. Ortiz De Montellano (Ed.), *Cytochrome P450: Structure, Mechanism,*  
523 *and Biochemistry*, Kluwer Academic/Plenum Publishers, New York, 2005, pp. 183-245.
- 524 [21] Z. Mazerska, P. Sowiński, J. Konopa, Molecular mechanism of the enzymatic oxidation  
525 investigated for imidazoacridinone antitumor drug, C-1311, *Biochem. Pharmacol.* 66  
526 (2003) 1727-1736.
- 527 [22] T. A. Baillie, M. N. Cayen, H. Fouda, R. J. Gerson, J. D. Green, S. J. Grossman, L. J. Klunk,  
528 B. LeBlanc, D. G. Perkins, L. A. Shipley, Drug metabolites in safety testing, *Toxicol. Appl.*  
529 *Pharmacol.* 182 (2002) 188-196.
- 530 [23] A. Potęga, D. Garwolińska, A. M. Nowicka, M. Fau, A. Kot-Wasik, Z. Mazerska, Phase I  
531 and phase II metabolism simulation of antitumor-active 2-hydroxyacridinone with  
532 electrochemistry coupled on-line with mass spectrometry, *Xenobiotica* (2018) DOI:  
533 10.1080/00498254.2018.1524946.A.
- 534 [24] M. Trunzer, B. Faller, A. Zimmerlin, Metabolic soft spot identification and compound  
535 optimization in early discovery phases using MetaSite and LC-MS/MS validation, *J. Med.*  
536 *Chem.* 52 (2009) 329-335.
- 537 [25] H. Orhan, N. P. E. Vermeulen, Conventional and novel approaches in generating and  
538 characterization of reactive intermediates from drugs/drug candidates, *Curr. Drug Metab.*  
539 12 (2011) 383-394.
- 540 [26] J. J. Pitt, Principles and applications of liquid chromatography-mass spectrometry in clinical  
541 bioanalysis, *Clin. Biochem. Rev.* 30 (2009)19-34.
- 542 [27] F. P. Guengerich, Common and uncommon cytochrome P450 reactions related to  
543 metabolism and chemical toxicity, *Chem. Res. Toxicol.* 14 (2001) 611-650.
- 544 [28] W. Lohmann, U. Karst, Generation and identification of reactive metabolites by  
545 electrochemistry and immobilized enzymes coupled on-line to liquid chromatography/mass  
546 spectrometry, *Anal. Chem.* 79 (2007) 6831-6839.
- 547 [29] S. T. M. Orr, S. L. Ripp, T. E. Ballard, J. L. Henderson, D. O. Scott, R. S. Obach, H. Sun,  
548 A. S. Kalgutkar, Mechanism-based inactivation (MBI) of cytochrome P450 enzymes:





549 structure–activity relationships and discovery strategies to mitigate drug–drug interaction  
550 risks, *J. Med. Chem.* 55 (2012) 4896-4933.  
551 [30] W. Lohmann, U. Karst, Simulation of the detoxification of paracetamol using on-line  
552 electrochemistry/liquid chromatography/mass spectrometry, *Anal. Bioanal. Chem.* 386  
553 (2006) 1701-1708.

554 **Figure captions**

555 **Figure 1**

556 Molecular structure and atomic numbering of antitumor-active imidazoacridinone C-1311.

557 **Figure 2**

558 Schematic diagram of the approaches used to study drug or drug candidate metabolic  
559 reactions, and/or generation of metabolites. (A) *In vivo* / *in vitro* models; (B) An instrumental  
560 set-up used for the electrochemical simulation of phase I oxidative metabolism; (C) *In silico*  
561 prediction of sites of metabolism. See the text for a detailed description.

562 **Figure 3**

563 Representative ESI mass spectra of C-1311 phase I oxidative transformation in the EC reactor  
564 (A) cell off and (B) cell on (positive ionization mode).

565 **Figure 4**

566 Representative two-dimensional (2-D) mass voltammograms for the selected ions, resulting  
567 from the electrochemical oxidation of C-1311 at a glassy carbon working electrode (extracted  
568 ion intensity versus the progress of the electrochemical oxidation; positive ionization mode).  
569 The *m/z* ratios shown correspond to the protonated [M+H]<sup>+</sup> C-1311 (*m/z* 351) and its putative  
570 products (see legend), and have been rounded to the nearest integer. The signal is dependent  
571 on the voltage used in the EC reactor (two and a half EC cycles are shown – see graph A)  
572 Experimental conditions: potential range 0 – 2.5 V; scan rate 10 mV s<sup>-1</sup>, continuous; T = 21 °C;  
573  $\phi$  glassy carbon working electrode 8 mm.

574 **Figure 5**

575 Extracted ion chromatograms of the selected mass ions, found in the mixture of C-1311 and  
576 its putative oxidation products leaving the electrochemical cell (extracted ion intensity versus  
577 the retention time; positive ionization mode). The *m/z* ratios shown have been rounded to the  
578 nearest integer. Peak names correspond to compounds presented in Table 2.

579 **Figure 6**

580 Representative Q-TOF-MS/MS spectra of the selected products of C-1311 electrochemical  
581 oxidation with proposed fragmentation assignments (insets). Q-TOF-MS/MS, quadrupole-time  
582 of flight-tandem mass spectrometry.

583 **Figure 7**

584 General overview of the proposed pathways of C-1311 electrochemical oxidation. Product  
585 structures were derived on the basis of measured masses and MS/MS fragmentation patterns.  
586 Product names correspond to compounds presented in Table 2.

**Figure 1**

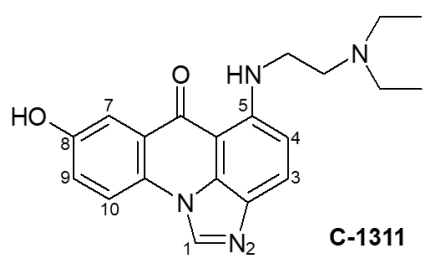


Figure 2

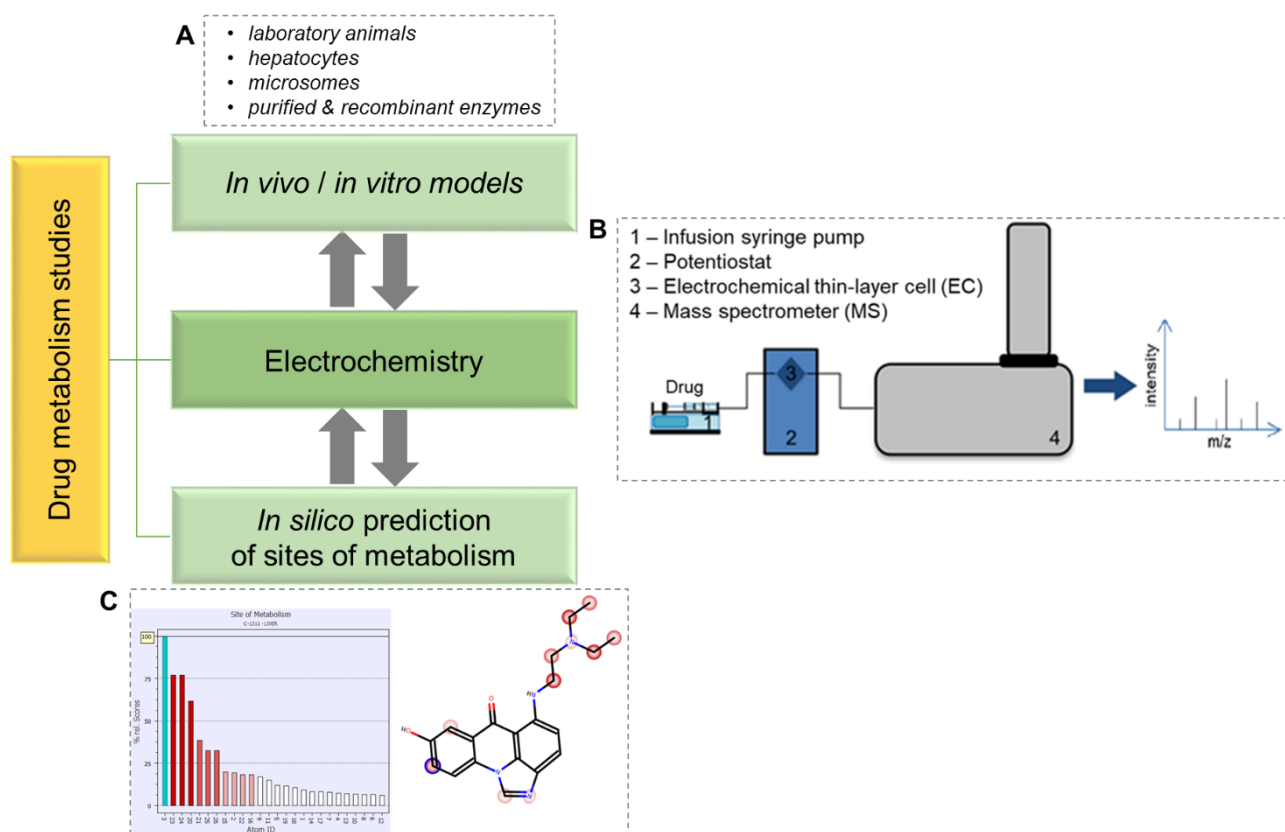


Figure 3

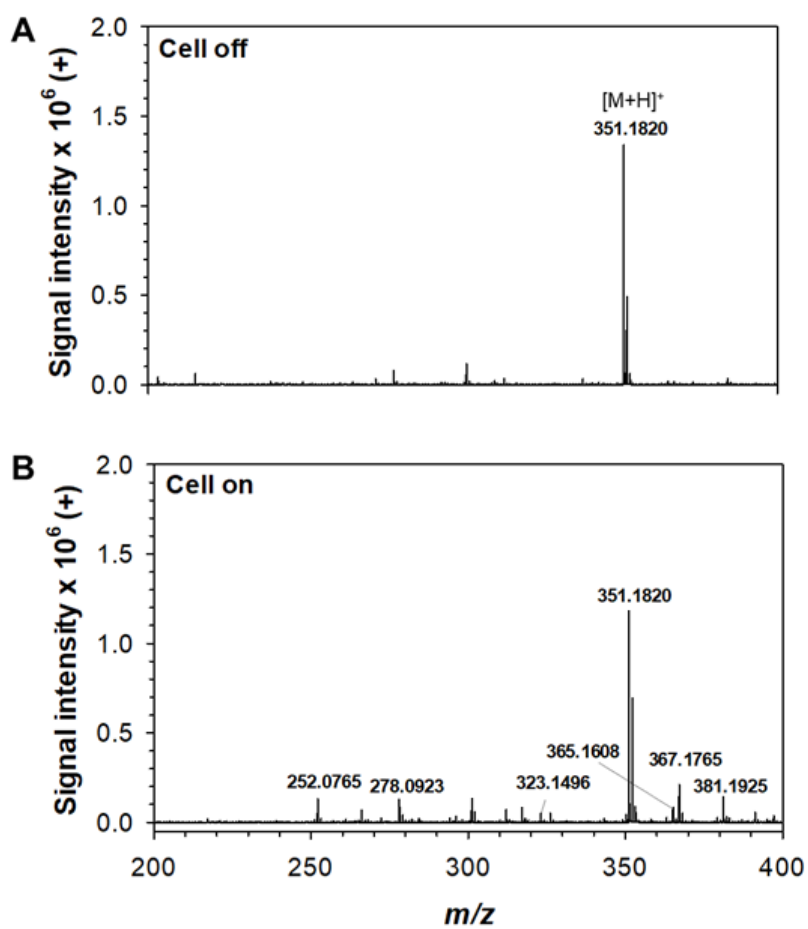


Figure 4

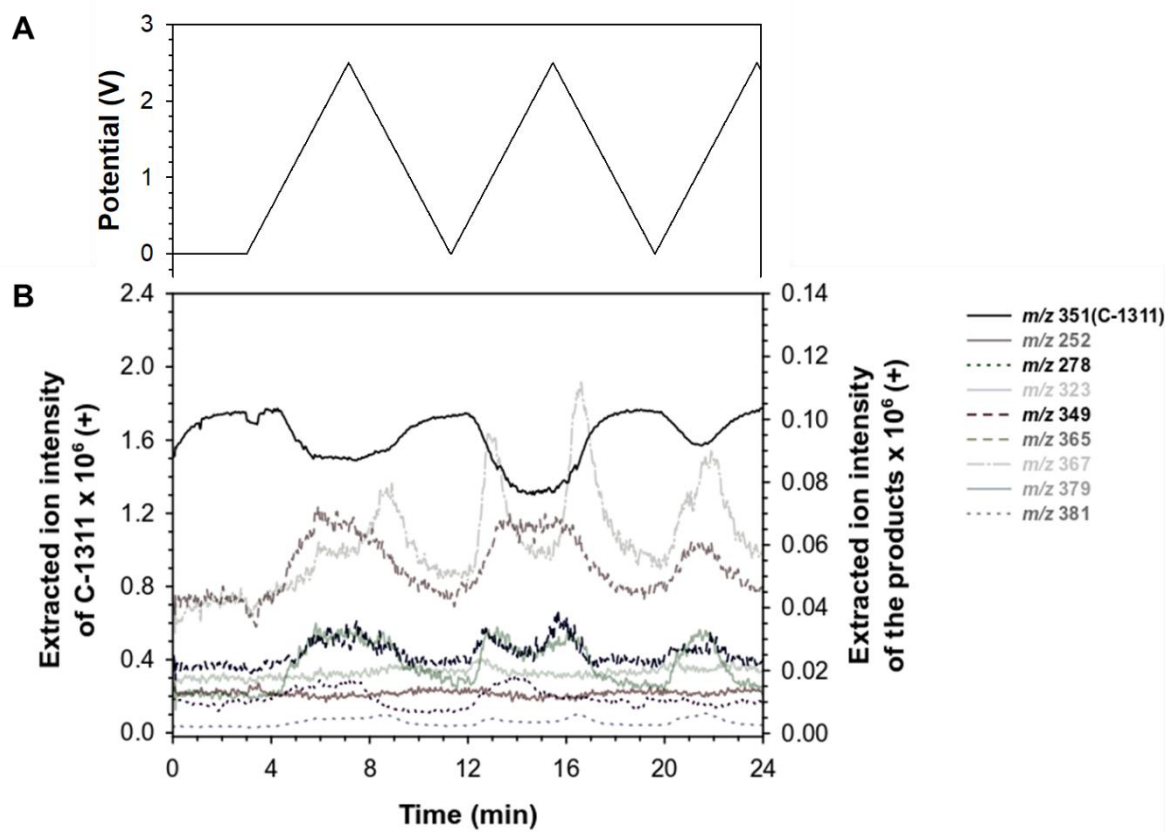


Figure 5

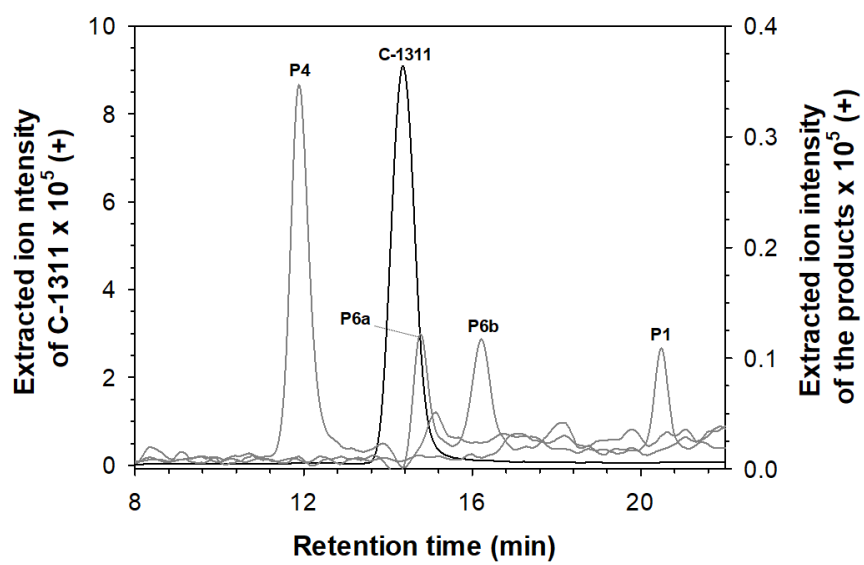




Figure 6

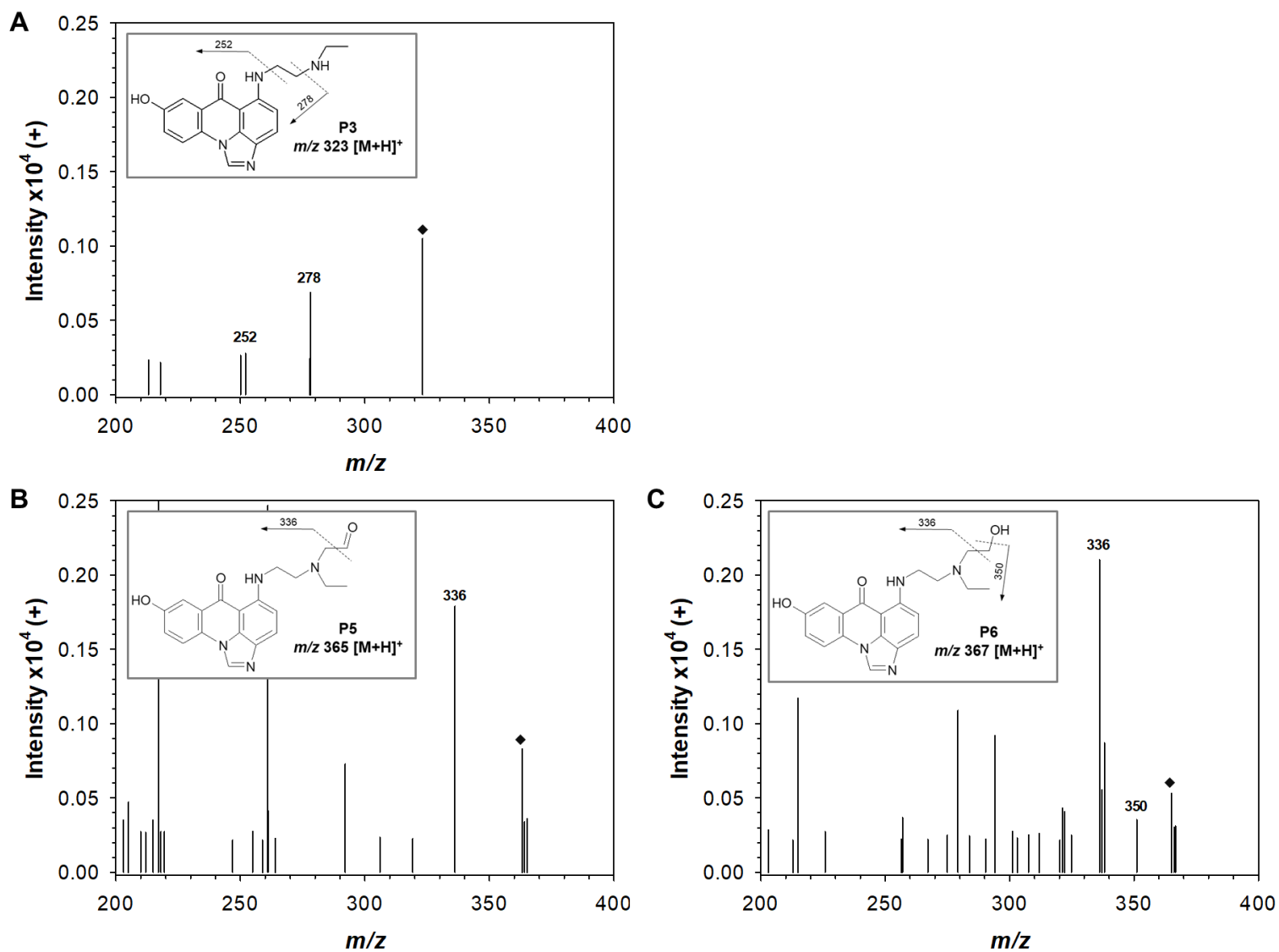
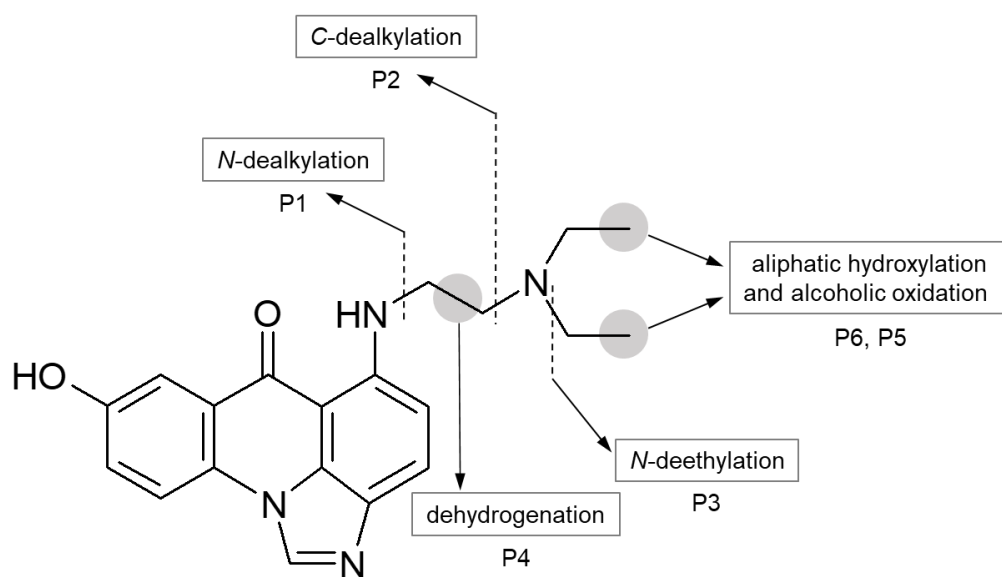


Figure 7



**Table 1**

EC, ESI-Q-TOF-MS, and ESI-ion trap MS/MS parameters as applied in direct EC/MS(/MS) experiments for determination of accurate masses of product ions and getting ion fragmentation.

	Parameter	Value or setting
EC settings	Flow rate	30 $\mu\text{L min}^{-1}$
	Potential	0 – 2.5 V (10 mV steps)
	EC operating mode	Scan
	Cycle	Continuous
MS(/MS) settings	Ion source	Dual electrospray
	MS operating mode	Scan
	Ion polarity	Positive
	The range of $m/z$	50 – 600
	Capillary voltage	3500 V
	Nebulizer gas ( $\text{N}_2$ ) pressure	35 psig
	Drying gas ( $\text{N}_2$ ) flow	10 $\text{L min}^{-1}$
	Drying gas temperature	325 $^{\circ}\text{C}$
	Fragmentor	175 V
	Skimmer	45 V
	OCT 1 RF Vpp	750 V
	Rate	1,5 spectra $\text{s}^{-1}$
	MS/MS method	targeted
	- Slope	- 4 $m/z$
- Offset	- 5 V	

**Table 2**

Accurate mass ion data and elemental composition changes associated with C-1311 products detected following electrochemical oxidation of the compound at a glassy carbon working electrode in a potential range of 0 – 2.5 V versus Pd/H<sub>2</sub>.

Name	Retention time (min)	Representative <i>m/z</i> [M+H] <sup>+</sup>	Mass error <sup>a</sup> (ppm)	Elemental composition	Elemental composition change	Transformation of C-1311
<b>C-1311</b>	14.33	351.1820	1.3	C <sub>20</sub> H <sub>22</sub> N <sub>4</sub> O <sub>2</sub>	-	-
P1	20.47	252.0765	-1.0	C <sub>14</sub> H <sub>9</sub> N <sub>3</sub> O <sub>2</sub>	- C <sub>6</sub> H <sub>13</sub> N	<i>N</i> -dealkylation (complete)
P2	ND <sup>b</sup>	278.0923	0.0	C <sub>16</sub> H <sub>11</sub> N <sub>3</sub> O <sub>2</sub>	- C <sub>4</sub> H <sub>10</sub> N	C-dealkylation
P3	Trace <sup>c</sup>	323.1496	-2.0	C <sub>18</sub> H <sub>18</sub> N <sub>4</sub> O <sub>2</sub>	- C <sub>2</sub> H <sub>4</sub>	<i>N</i> -deethylation
P4	11.88	349.1665	1.7	C <sub>20</sub> H <sub>20</sub> N <sub>4</sub> O <sub>2</sub>	- 2H	dehydrogenation
P5	ND <sup>b</sup>	365.1608	0.0	C <sub>20</sub> H <sub>20</sub> N <sub>4</sub> O <sub>3</sub>	+ O - 2H	oxidation
P6a, b	14.79; 16.22	367.1765	0.1	C <sub>20</sub> H <sub>22</sub> N <sub>4</sub> O <sub>3</sub>	+ O	hydroxylation/ <i>N</i> -oxidation
P7	ND <sup>b</sup>	379.1764	0.0	C <sub>21</sub> H <sub>22</sub> N <sub>4</sub> O <sub>3</sub>	+ O - 2H + CH <sub>2</sub>	oxidation + methylation
P8	Trace <sup>c</sup>	381.1925	1.0	C <sub>21</sub> H <sub>24</sub> N <sub>4</sub> O <sub>3</sub>	+ O + CH <sub>2</sub>	hydroxylation + methylation

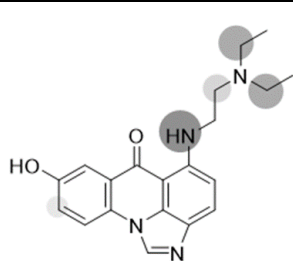
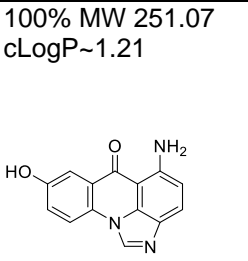
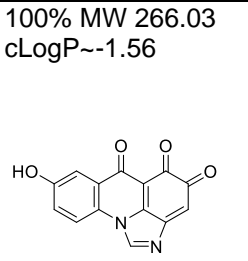
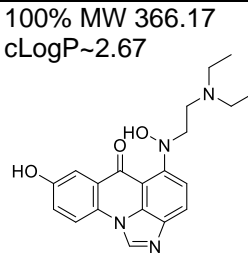
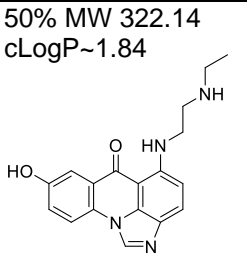
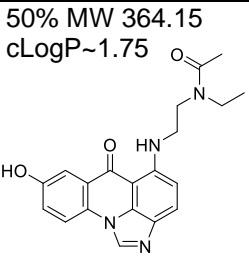
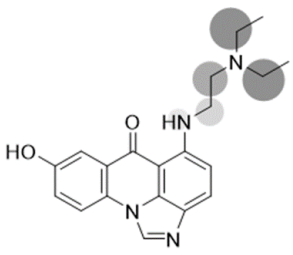
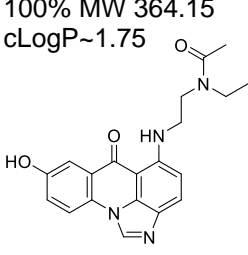
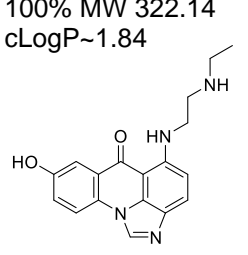
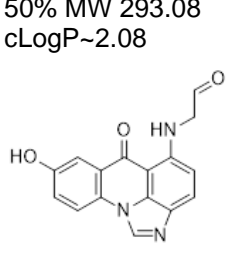
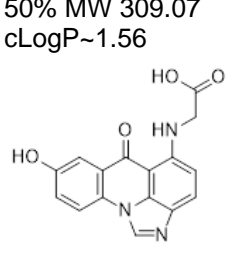
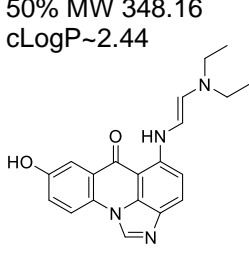
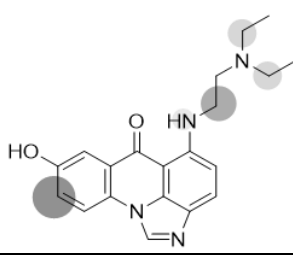
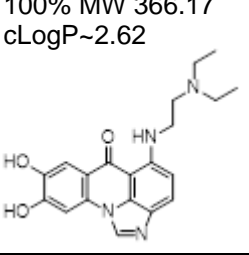
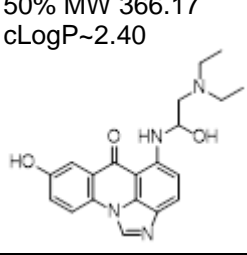
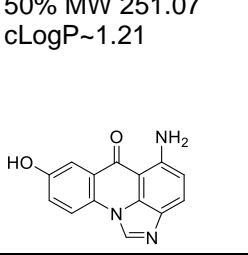
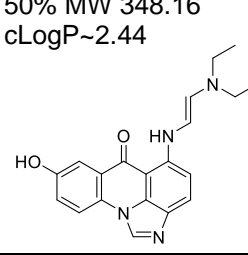
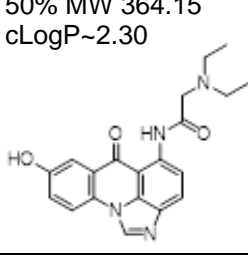
<sup>a</sup> Exact masses were calculated using Molecular Mass Calculator freeware version v2.02.

<sup>b</sup> ND, not detected.

<sup>c</sup> Trace, trace amounts observed.

**Table 3**

Most probable sites of metabolism (SoMs) and top ranked P450 1A2-, and 3A4- and 2D6-mediated metabolites predicted for C-1311 using MetaSite software.

SoMs for C-1311 (MW 350.17, cLogP 2.78)		Most probable metabolites predicted (n = 5 for P450 1A2 and 2D6, n = 6 for P450 3A4) and respective likelihood ranking					
P450 1A2		100% MW 251.07 cLogP~1.21 	100% MW 266.03 cLogP~-1.56 	100% MW 366.17 cLogP~-2.67 	50% MW 322.14 cLogP~-1.84 	50% MW 364.15 cLogP~-1.75 	
	P450 3A4		100% MW 364.15 cLogP~-1.75 	100% MW 322.14 cLogP~-1.84 	50% MW 293.08 cLogP~-2.08 	50% MW 309.07 cLogP~-1.56 	50% MW 348.16 cLogP~-2.44 
P450 2D6		100% MW 366.17 cLogP~-2.62 	50% MW 366.17 cLogP~-2.40 	50% MW 251.07 cLogP~-1.21 	50% MW 348.16 cLogP~-2.44 	50% MW 364.15 cLogP~-2.30 	

The functional groups that most likely will be metabolized are marked: the darker the color and the greater the circle of marked functional group – the higher the probability of metabolism to occur. MW, molecular weight; cLogP, the logarithm of partition coefficient.

**Table 4**

Representation of putative oxidative products of C-1311 and their detection in various *in vitro* metabolism generation platforms or predicted with the use of MetaSite. The *m/z* ratios shown have been rounded to the nearest integer.

<i>m/z</i> of putative metabolite	Occurrence or predicted by					
	EC	<i>In vitro</i>		<i>In silico</i> (MetaSite)		
		RLMs or HLMs [7]	HRP/H <sub>2</sub> O <sub>2</sub> [21]	P50 1A2	P450 3A4	P450 2D6
252	+	-	+	+	-	+
278	+	-	-	-	-	-
323	+	+	+	+	+	-
349	+	-	-	-	+	+
365	+	-	-	+	+	+
367	+	+	-	+	-	+
379	+	-	-	-	-	-
381	+	-	-	-	-	-

EC, electrochemistry reaction in ROXY™ system; RLMs, rat liver microsomal incubations; HLMs, human liver microsomes; HRP/H<sub>2</sub>O<sub>2</sub>, horseradish peroxidase/hydrogen peroxide.

